AD-A142 790 PERFORMANCE RESULTS OF A SMALL-CALIBRE ELECTROMAGNETIC LAUNCHER(U) MATERIALS RESEARCH LABS ASCOT VALE (AUSTRALIA) G A CLARK ET AL. FEB 84 MRL-R-917 1/1

UNCLASSIFIED F/G 21/3 NL

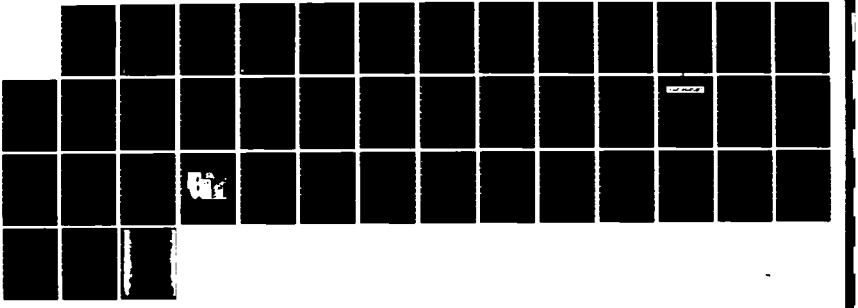

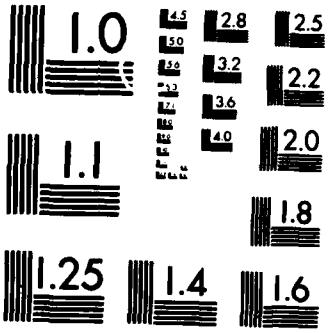

MRL-R-917

AR-003-898

(12)

DEPARTMENT OF DEFENCE

DEFENCE SCIENCE AND TECHNOLOGY ORGANISATION

MATERIALS RESEARCH LABORATORIES

MELBOURNE, VICTORIA

REPORT

MRL-R-917

PERFORMANCE RESULTS OF A SMALL-CALIBRE ELECTROMAGNETIC LAUNCHER

G.A. Clark & A.J. Bedford

Approved for Public Release

FEBRUARY, 1984

DEPARTMENT OF DEFENCE

MATERIALS RESEARCH LABORATORIES

REPORT

MRL-R-917

PERFORMANCE RESULTS OF A SMALL-CALIBRE ELECTROMAGNETIC LAUNCHER

G.A. Clark & A.J. Bedford

ABSTRACT

Results of electromagnetic launcher experiments are presented. Using an inductor and a crowbarred capacitor bank, 0.3 g projectiles have been accelerated over 800 mm to a velocity of 3.3 km/s. Voltage, current, power and energy curves are presented, as are tables of muzzle volts and efficiencies. The launcher design, circuit parameters and instrumentation are detailed and discussed. The report has been presented in a manner such that the data may be used by others to test theoretical work and to compare with experiments on other systems.

POSTAL ADDRESS: Director, Materials Research Laboratories
P.O. Box 50, Ascot Vale, Victoria 3032, Australia

SECURITY CLASSIFICATION OF THIS PAGE UNCLASSIFIED

DOCUMENT CONTROL DATA SHEET

REPORT NO.	AR NO.	REPORT SECURITY CLASSIFICATION
MRL-R-917	AR-003-898	UNCLASSIFIED

TITLE

PERFORMANCE RESULTS OF A SMALL-CALIBRE ELECTROMAGNETIC LAUNCHER

AUTHOR(S)

G.A. CLARK
A.J. BEDFORD

CORPORATE AUTHOR
Materials Research Laboratories
P.O. Box 50,
Ascot Vale, Victoria 3032

REPORT DATE	TASK NO.	SPONSOR
FEBRUARY 1984	DST 82/212	DSTO

CLASSIFICATION/LIMITATION REVIEW DATE

CLASSIFICATION/RELEASE AUTHORITY
Superintendent, MRL
Physical Chemistry Division

SECONDARY DISTRIBUTION

Approved for Public Release

ANNOUNCEMENT

Announcement of this report is unlimited

KEYWORDS

Electric guns Railguns

COSATI GROUPS 2103 1906

ABSTRACT

Results of electromagnetic launcher experiments are presented. Using an inductor and a crowbarred capacitor bank, 0.3 g projectiles have been accelerated over 800 mm to a velocity of 3.3 km/s. Voltage, current, power and energy curves are presented, as are tables of muzzle volts and efficiencies. The launcher design, circuit parameters and instrumentation are detailed and discussed. The report has been presented in a manner such that the data may be used by others to test theoretical work and to compare with experiments on other systems.

CONTENTS

LIST OF FIGURES

LIST OF TABLES

PERFORMANCE RESULTS OF A SMALL-CALIBRE ELECTROMAGNETIC LAUNCHER

1. INTRODUCTION

The rail-gun electromagnetic launcher has been proposed as a method by which electromagnetic forces may be harnessed to propel projectiles to velocities from 2 to perhaps hundreds of km/s [1,2,3]. Theoretical analyses and results from current research indicate that this means of propulsion is not limited by the velocity of sound as is the case for chemical propellants. Electromagnetic launchers which can efficiently propel projectiles to extremely high velocities will have military applications in such areas as point defence, anti-armour and anti-missile defence. Field guns may be developed with greater range and accuracy due both to higher muzzle velocities and greater control over muzzle velocity. Other research also indicates that large payloads may be launched by electromagnetic means to have uses in surveillance and supply delivery, and in the case of naval forces, for catapults on aircraft carriers and perhaps for torpedo launch. Industrial and scientific applications are foreseen in such areas as space launch, metal processing, equation of state research, and perhaps even as a means of generating electrical power via impact fusion.

Rashleigh and Marshall [1] at the Australian National University (ANU) demonstrated the feasibility of railgun accelerators and in some experiments used a plasma rather than a solid conducting armature, the principal features of which are shown in figure 1. Current work at MRL

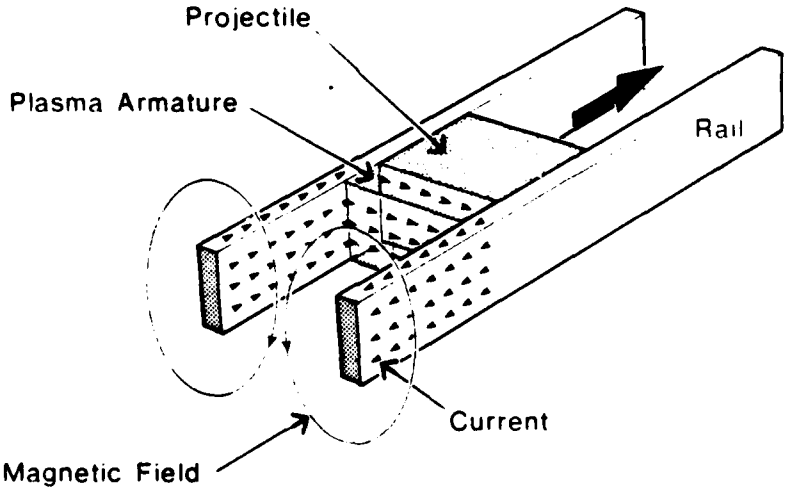

FIGURE 1 Characteristics of a plasma driven railgun

is directed towards understanding and characterising such plasma armatures which are used to push projectiles to hyper velocities. Theoretical modelling by Thio [4] resulted in a simulation code called PARA ("Plasma Armature Railgun Accelerator"). The code is dynamic as the state of the plasma is allowed to vary with time. The impedance of the plasma is combined with the impedances of the busbars, the rails and the power source in the circuit equation. When combined with the equations of motion the dynamic parameters of the launcher are determined.

Some of the experimental program at MRL has been based on simulations using the PARA code. A number of differently constructed rail-type accelerators have been employed [5] and this paper details the results of the device designated ERGS-1M where the acronym "ERGS" means "Experimental Rail-Gun System".

2. CIRCUIT DESCRIPTION

Figure 2 shows the experimental arrangement of the capacitor bank, large loop indicator, spark gap switches and the barrel. Details and specifications of the components used in these and other small calibre railgun experiments are given in references 5 and 6.

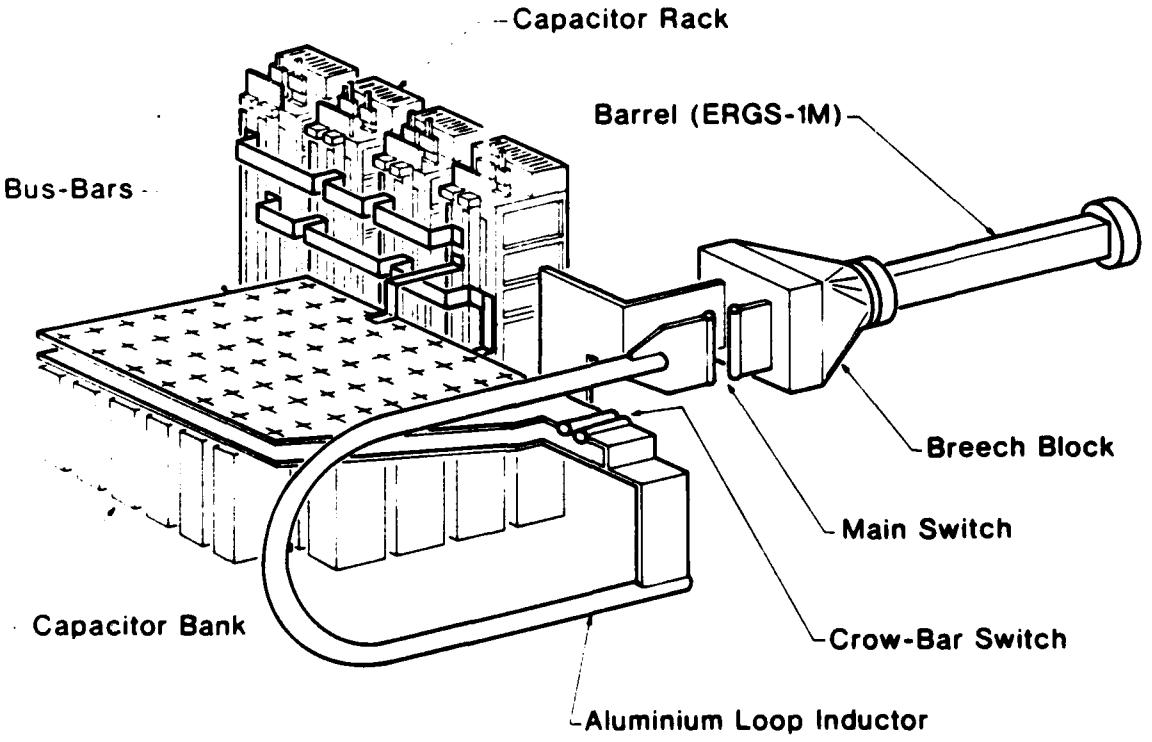

FIGURE 2 Arrangement of the Experimental Rail Gun System (ERGS)

2.1 Capacitor Bank

Figure 3 shows the circuit for the launcher. The capacitor bank was composed of thirty four 78 μF BICC capacitors paralleled with a further eighteen 200 μF Maxwell capacitors.

The inductance and resistance of the bank was measured at 909 Hz which was close to the fundamental frequency of the circuit.

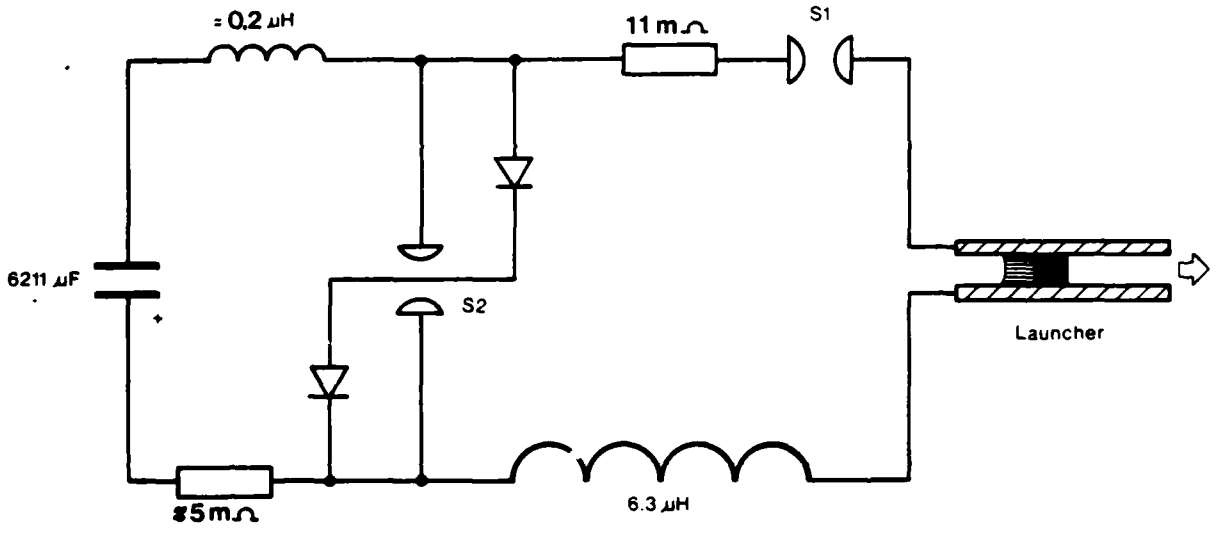

FIGURE 3 Circuit diagram for the ERGS-1M system showing component values and circuit resistances

2.2 Inductor

The storage inductor was a single elongated loop of 50 mm diameter aluminium bar held in a wooden frame [5]. The inductance and resistance were measured at a frequency of 909 Hz and found to be 6.3 μH and 1.2 m Ω respectively.

2.3 Switches

Two simple arc switches were designed and constructed [5,6]. The main switch (S1, Fig. 3) consists of two copper-tungsten (75%W, 25%Cu) electrodes aligned parallel and opposite each other, the space between them being a break in the circuit. To close the switch a spring loaded perspex plunger tipped with aluminium foil was released into the gap.

The crowbar switch (S2, Fig. 3) was of similar design to the main switch and was positioned across the narrow end of the capacitor bank transmission plates. A copper wire (0.05mm diameter, 80mm long) was positioned on the central plane of the 4mm spacing of the electrodes, and each end of the wire was connected via a diode to a transmission plate. Upon closure of the main switch the reversing of the capacitor voltage after a quarter cycle forward biased the diodes and exploded the copper fuse wire. The copper plasma filling the crowbar switch gap initiated switch closure.

3. LAUNCHER COMPONENTS

3.1 Launcher Body and Rails

The body of the launcher (Fig. 4) was a fibre-glass epoxy-resin composite qualified under MIL-P-18177-GEB. The launcher may be breech or muzzle loaded and have either an open or closed breech. All results presented are for an open breech.

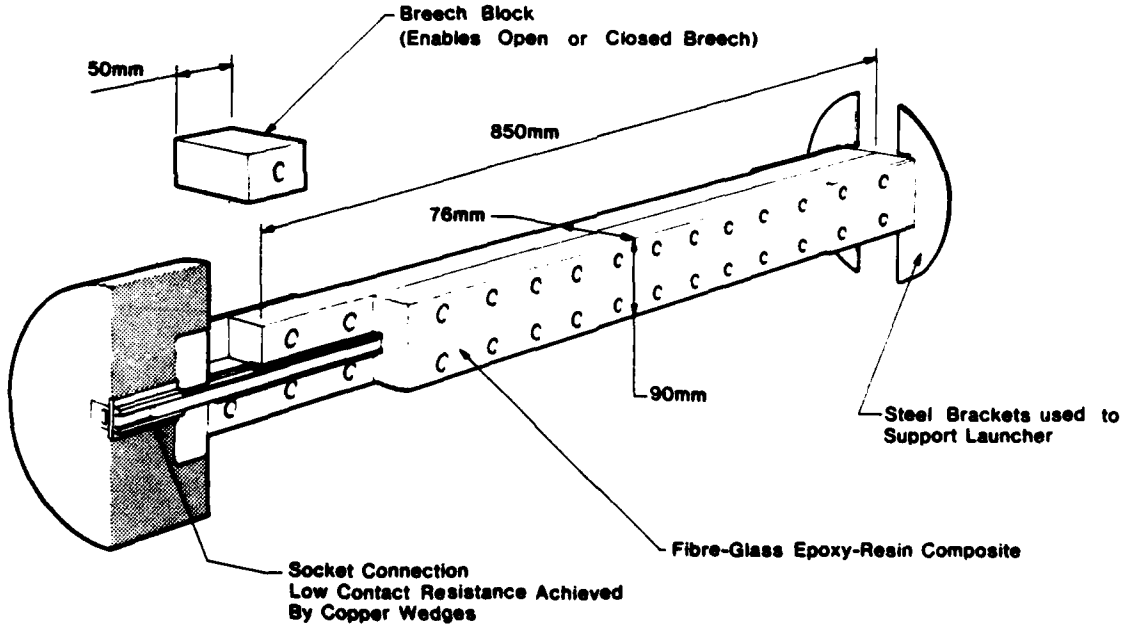

FIGURE 4 ERGS-1M Barrel and Breech Assembly

Attachment of the launcher to the busbars was by a plug and socket arrangement. Pressure was applied to the junction by internal copper wedges. This particular design was adopted so that the barrel could be evacuated, however the tests reported herein were all conducted at atmospheric pressure.

The railgun bore size was 6.00 mm high and 7.90 mm wide. The rails were 10 x 5 mm copper - 0.6% cadmium in the extruded work hardened condition. After each firing the rails were removed for metallurgical examination and a new set installed. The dielectric wall of the bore was a vulcanised cellulose fibre [5].

3.2 Railgun Inductance

The inductance per unit length (L') of the rails in a railgun is one of the most important parameters to be considered, indeed its actual value during railgun firings is a subject of some speculation [7]. To select a value for our calculations of railgun performance, inductance was measured over a frequency range from 451 Hz to 20 kHz, both with the barrel fully assembled and with bolts and mounting brackets removed. Variation in the inductance was expected due to the proximity effect, and the varying skin depth in the rails together with the generation of eddy currents in any nearby metal components.

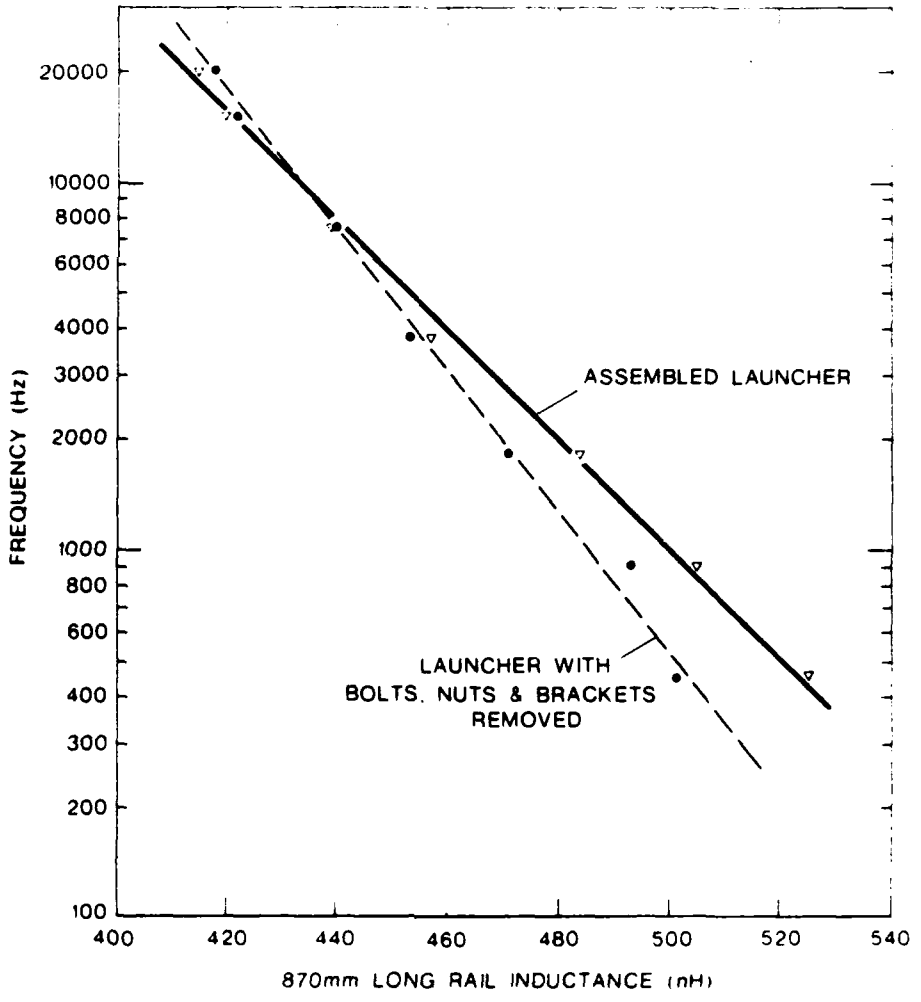

FIGURE 5 Variation of Total Railgun inductance with respect to frequency

It can be seen from Fig. 5 that the presence of the bolts and brackets alters L' but the maximum difference was less than 4%. An interesting feature is that the inductance against frequency plots are straight lines but they are not parallel. A cross-over occurs at about 9.5 kHz.

To measure these inductance values a shorting link was used at the rail ends. The effect on inductance of this link was determined by taking measurements on different length rail sets, and its inductance was determined to be 20 nH. From the experimentally measured gun inductance at 909 Hz (approximately the fundamental frequency of the railgun circuit), the L' was then calculated to be 0.54 μH/m.

3.3 Projectile

Projectiles (fig. 6) were made from vulcanised cellulose fibre, the same dielectric material used for the rail spacers. To avoid shearing, the principal fibre direction of the material was oriented 90 degrees to the direction of acceleration.

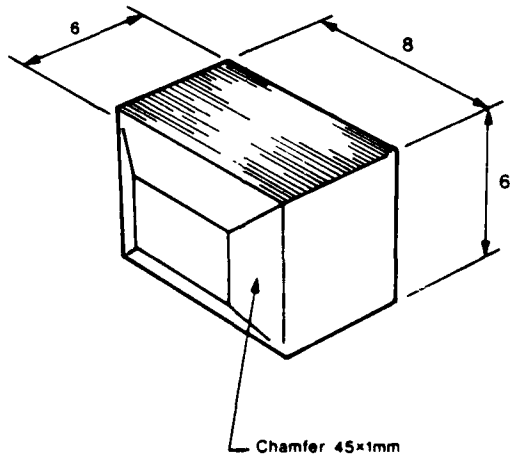

FIGURE 6 Projectile Design with Nominal Dimensions

Clearance around the projectile was designed to be from 0.005 mm to 0.035 mm. However due to the flatness tolerance (0.012 mm) of the unmachined extruded rails some projectiles had to be rubbed on 600 grit carbide paper to obtain a good sliding fit within the bore. The parallel tolerance of the extruded rails was ± 0.005 mm.

Each projectile was weighed before and after the foil was attached. Average projectile mass was 0.31 ±0.01 g (without the glue and foil).

Muzzle loading was used for every firing to ensure that the foil had good contact with both rails. Shorting of the rails by the foil was checked with an ohmmeter before each firing.

3.4 Foil Fuse

Commonly available domestic aluminium foil (>99.5% pure) was used on the rear of the projectile. The foil, 0.05mm thick was cut into a rectangle 44mm x 6mm and folded in half lengthwise twice. The foil, now 11mm x 6mm, was glued to the chamfered face of the projectile with cyanoacrylate adhesive. The average mass of the foil was 0.011 ±0.001 g. The average additional mass of the glue used was 0.006 g.

4. DATA ACQUISITION

4.1 Voltage Records

Each voltage was captured with a Datalab 910 transient recorder. Every recorder measuring voltage was electrically floated with mains power being supplied via isolation transformers. Attachment of the recorders to the launcher was via Tektronix P6015 HV probes.

All recorders were externally triggered by opto-isolators, the initial trigger pulse being derived from a 300 mm diameter coil placed in the inductor. By using the pre-trigger facility of the recorders, data before the trigger pulse were also captured.

Table 1 lists the measured electrical parameters.

T A B L E 1

PARAMETER	SAMPLING RATE OF DATALAB DL 910 TRANSIENT RECORDERS
Capacitor voltage	0.5 µs
Current	"
Muzzle voltage	"
Breech voltage	"
Position coils	0.2 µs
Position coils	"

Each record of 4096 bytes captured by the recorders was accessed by a PDP 11/23 mini computer via an IEEE 488 data bus and stored on hard disk with floppy disk backup.

4.2 Velocity

A calibrated ballistic pendulum placed 2 metres from the muzzle recorded the momentum of the projectile from which the velocity was determined. A thin paper witness screen on the front of the pendulum confirmed whether the projectile was intact or broken at the instant of hitting the pendulum. Table 3 (page 10) lists the velocities determined from the pendulum.

5. RESULTS

Of the 12 scheduled firings ranging in voltage between 3.0 and 7.0 kV, there were 10 firings from which data were successfully recorded. Table 2 lists the firings.

T A B L E 2

FIRING NO.	VOLTAGE (kV)	COMMENTS	*ENERGY EXPENDED (kJ)
1	6.0	-	112.1
2	4.2	Premature firing of main switch	54.8
3	6.0	-	111.8
4	7.0	78 µF capacitor failure	-
5	4.2	-	54.1
6	5.0	-	76.7
7	5.0	-	76.7
8	7.0	Crowbar switch failure	-
9	7.0	Cracks appeared in launcher body	150.3
10	3.0	2 mm lengthening of crack	27.8
11	3.0	-	28.0
12	7.0	Significant crack displacement	149.4

* Energy expended is the initial stored energy in the capacitors minus the residual energy remaining after the firing.

5.1 Capacitor Voltage

Fig 7 displays the curve for firing number 12; it shows the DC voltage of the charged bank, a spike at the closure of the main switch, the sinusoidal decay to zero and voltage reversal leading to crowbarring. From the instant of crowbar there is a low amplitude oscillation in the reversal region. The residual voltage on the capacitor after the discharge was 180 volts. Table 3 (page 10) lists the initial and residual capacitor voltages of each firing.

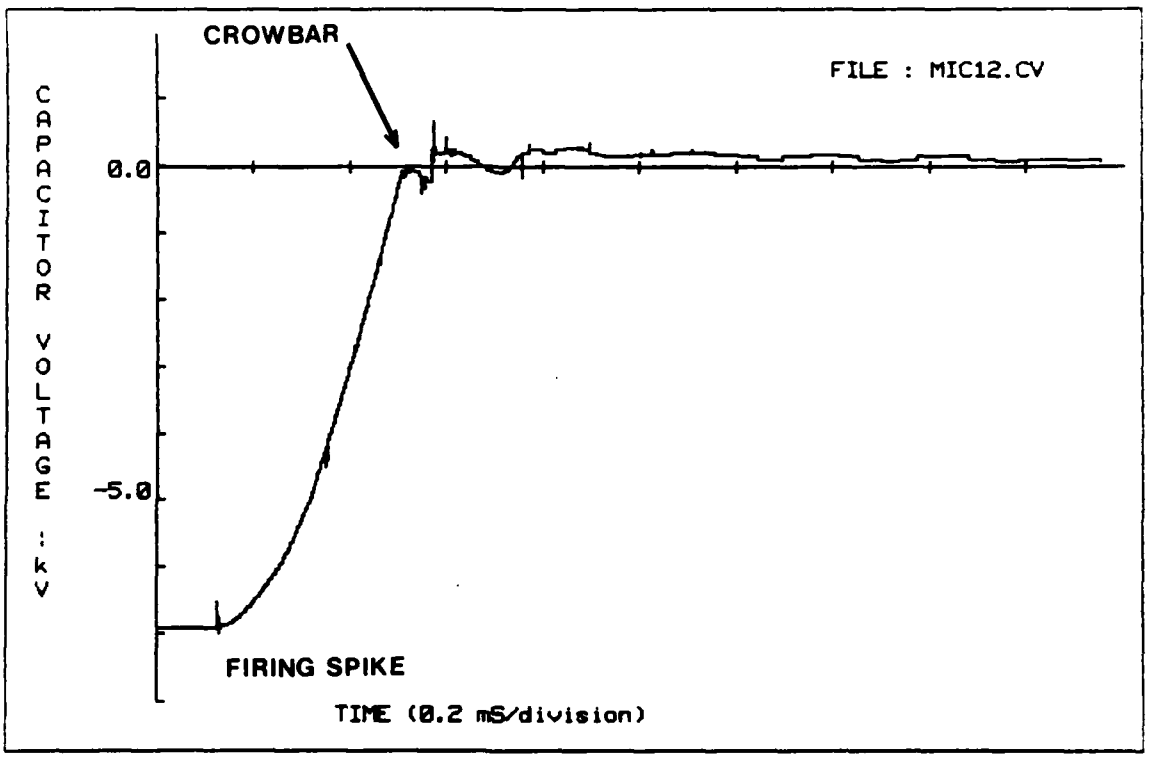

FIGURE 7 Capacitor voltage for firing No. 12

5.2 Current

Current was measured by a Rogowski belt (Appendix A) connected via a simple RC integrator to a transient recorder. The time constant of this integrator introduced an appreciable error in the records. Analysis of the circuit (Appendix B) enabled this error to be calculated and the records to be corrected. The sensitivity of the belt was 92 ±10 kA/volt. Figure 8 shows the uncorrected and corrected current curves for firing number 12. Similar to the voltage curve there is a DC level before firing (on uncorrected raw data curve) a switching spike and the sinusoidal climb in current. Upon reaching a peak of 147 kA the current starts a sinusoidal decay. During this decay the crowbar switch is closed, indicated by a spike in the trace and an exponential decay begins.

TABLE 3

Firing No.	CAPACITOR VOLTAGE		Total Energy Expended	Breech Energy Up to Proj. exit	Projectile Velocity	Projectile Kinetic Energy	System Efficiency	Launcher Efficiency
	Initial Voltage (kv)	Residual Voltage (V)	(kJ)	(kJ)	(km/s)	(kJ)	(%)	(%)
10	3.0	20	27.8	9.1	1.5	0.34	1.2	3.7
11	3.0	60	28.0	8.9	1.5	0.34	1.2	3.8
2	4.2	0	54.8	12.9	2.7	1.13	2.1	8.8
5	4.2	94	54.1	13.4	2.5	0.97	1.8	7.2
6	5.0	100	76.7	17.4	2.8	1.22	1.6	7.0
7	5.0	100	76.7	18.4	2.8	1.17	1.5	6.4
1	6.0	157	112.1	22.7	2.9	1.27	1.1	5.6
3	6.0	23	111.8	-	3.2	1.60	1.5	-
9	7.0	180	150.3	28.3	3.3	1.63	1.1	5.8
12	7.0	207	149.4	26.0	2.5	0.93	0.6*	3.6*

*Significant crack in launcher body.

Close examination of the exponential decay portion of the curve shows a decrease in gradient occurs at the exit of the plasma armature. The change indicates an increase in the resistivity of the plasma. This is probably due to the expansion of the plasma after exiting the launcher as the residual energy in the system is dissipated across the muzzle.

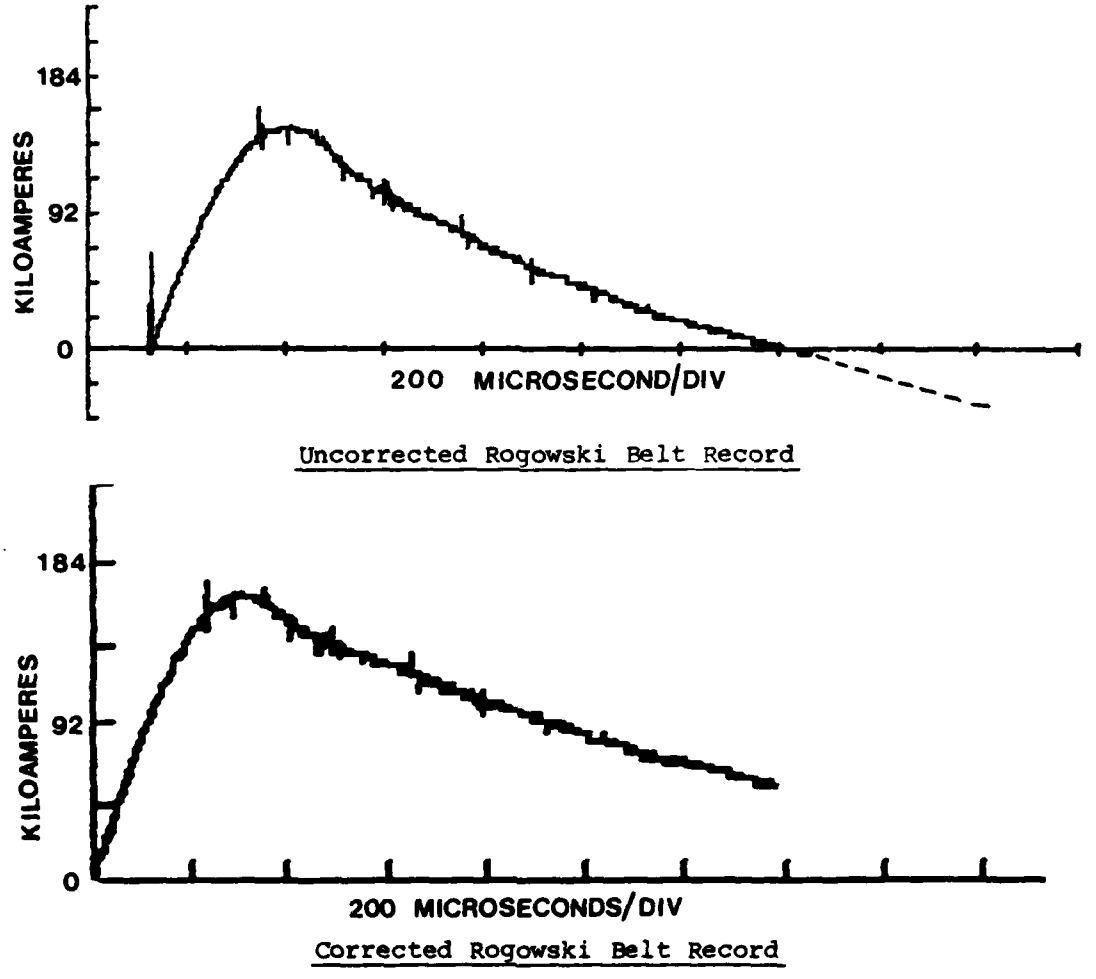

FIGURE 8 Comparison of uncorrected and corrected Rogowski Belt Signals, (Firing No. 12).

5.3 Muzzle Voltage

Figure 9 displays a typical muzzle voltage record (firing No.11). This in effect is the voltage across the plasma armature which also includes any plasma-rail interface voltage drops. Features are the zero voltage before firing, the firing spike and a fast rising spike (as the foil is heated and exploded) which falls quickly to a trough. This is followed by a small peak, a trough and then a slow sinusoidal rise to a peak which falls to a "plateau". One of the spikes around this region is due to the crowbar switch closure. Following this voltage plateau there is a sharp rise in voltage indicating the exit of the plasma from the launcher.

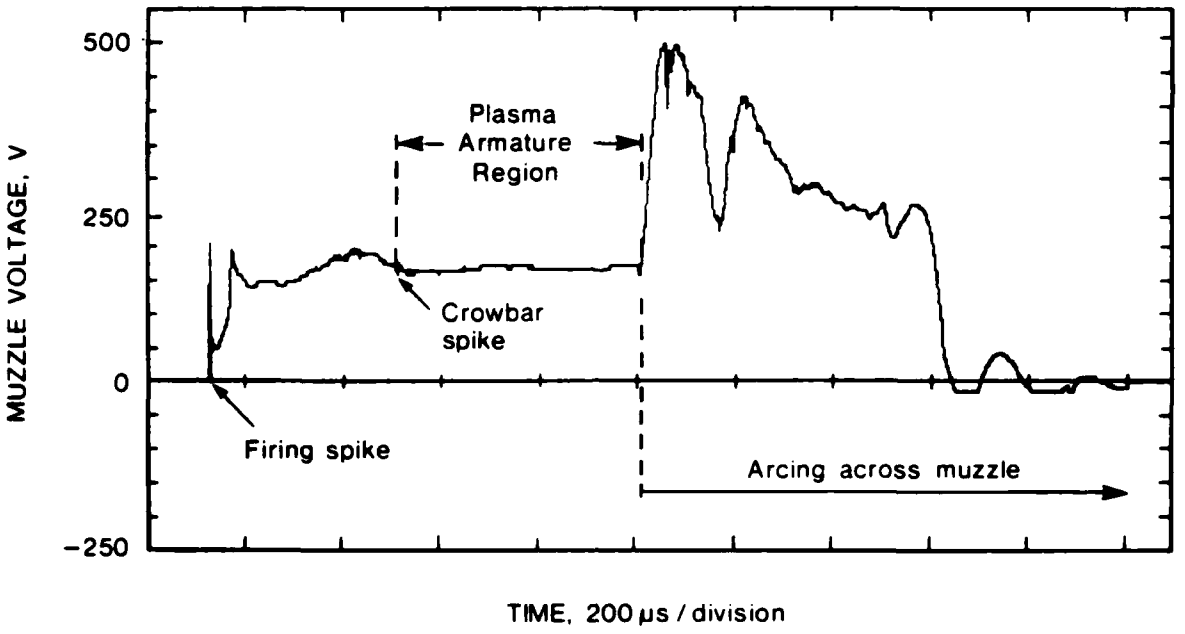

FIGURE 9 Muzzle voltage record for firing No. 11. Capacitor bank voltage was initially 3 kV

We have defined the interval from crowbar to plasma exit as the "plasma armature" region ie the inductively driven region. By this time the plasma armature has been fully formed and the discharge appears to be stable. Of particular interest in this part of the firing is that the armature current may fall by a factor of two, while the muzzle voltage remains almost constant, or decreases slowly. The muzzle voltage may be expressed as;

$$V = IR_A + L_A\dot{I} + V_+ + V_-$$

Where....

I = armature current

R_A = plasma column resistance

L_A = inductance of plasma column

V_+, V_- = respective rail-plasma interface voltage drops

Within the initial region of the inductive driven discharge, $\dot{I}$ would be essentially constant and L_A is small. Therefore to explain the muzzle volts value with falling current, the plasma column resistance and/or the rail-plasma interface voltages must increase. If one assumes that the rail-plasma interface voltages are constant, then the resistivity of the plasma has to increase. This increase may be brought about by the cooling of the plasma as a result of the lower power input to the armature.

To further investigate the behaviour of the armature (muzzle) voltage the average values of this voltage (in the plasma armature region) were calculated from each firing. Simulation work has in general been conducted with the assumption of a constant value for the plasma voltage drop though there has been some contention that what happens in the plasma armature region depends upon the energy input to the launcher. To examine this Fig. 10 is a plot of the average plasma armature voltage against energy input to the launcher up to the instant of crowbar switch operation (see Fig. 9 for reference points). Use of the energy expended up to operation of the crowbar switch may be thought of as a measure of energy to establish the stable driving plasma, but the choice is subjective and used here only to show that some energy input parameter probably influences the ultimate value of armature voltage. The plot indicates that as energy input increases, armature voltage increases, however, there are insufficient results to determine the full nature of the curve and further experimentation is needed.

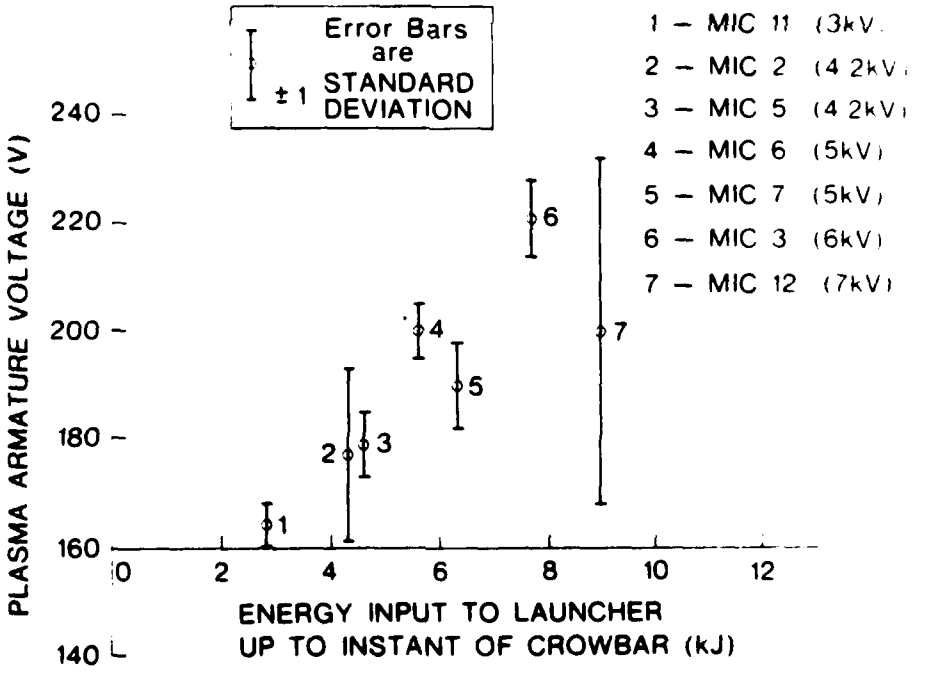

FIGURE 10 Variation of plasma armature voltage with respect to the energy input which formed the stable plasma armature region

The presence of the same early features in all of our records of muzzle voltages suggests to us that they are associated with fundamental processes in the formation of the plasma armature.

To pursue this belief, plots were made, on logarithmic scales, of the initial capacitor voltage against time to each of the first three characteristics labelled on Fig. 11(a). Straight line relationships are indicated, Fig. 11(b).

A possibility is that the initial rising spike is due to the increasing resistance of the foil as it is heated and vapourised with the subsequent fall in voltage being caused by the generation of plasma with lower resistance. But, at this stage the current is still increasing rapidly and it more than compensates for the resistance decrease and to a voltage increase occurs. However, if this explanation is correct, the voltage will determine the power input to the foil, and the characteristic intervals of time will be proportional to $1/V^2$. Our results show that the intervals are proportional to approximately $1/\sqrt{V}$. We therefore conclude that other phenomena are involved to result in this weak voltage dependence and better understanding of these processes will be needed to elucidate plasma formation and equilibrium conditions as well as associated rail damage mechanisms.

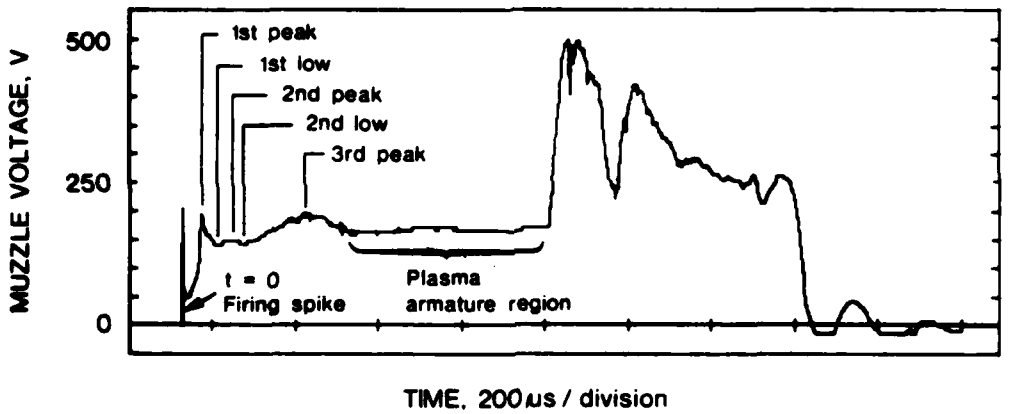

FIGURE 11(a) Observed characteristics of muzzle voltage records

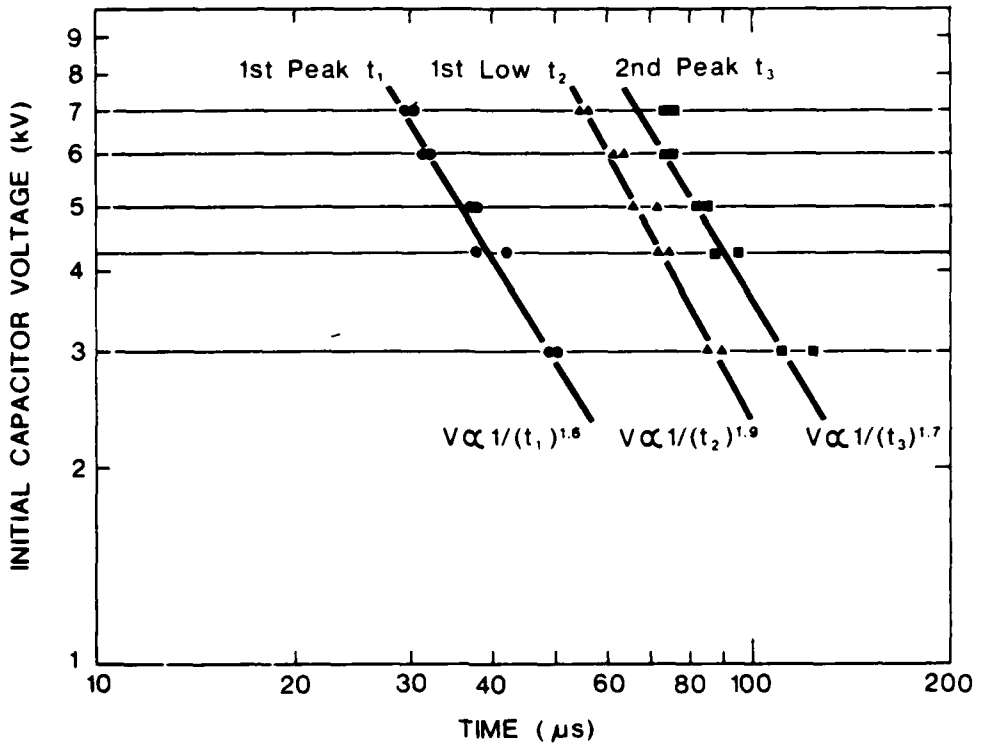

FIGURE 11(b) Initial capacitor voltage versus time of occurrence for 3 characteristic features of the muzzle voltage records

For completeness and so that others may use the data, Table 4 is presented for the current series of experiments.

T A B L E 4

MUZZLE VOLTS CHARACTERISTICS

Capacitor Voltage	3KV		4.2KV		5KV		6KV		7KV			
	Firing Number											
Characteristic	10	11	2	5	6	7	1	3	12	9	Units	+Mean ±1 S.D.
1st peak volts	-	192	261	349	298	325	388	290	224	-	volts	291V±65
" " time	*50.0	48.5	37.5	41.5	37.5	37.0	31.5	31.5	29.5	*30.0	µsecs	
1st low volts	-	137	147	149	153	149	161	164	149	-	volts	151V±8
" " time	*84.5	88.5	74.0	71.0	71.0	65.0	61.0	63.5	56.0	*54.0	µsecs	
2nd peak volts	-	145	163	192	165	180	180	184	169	-	volts	172V±15
" " time	*109.5	121.5	94.0	87.5	85.0	81.5	75.5	72.5	72.5	*75.0	µsecs	
2nd low volts	-	141	145	153	149	172	-	167	-	-	volts	155V±12
" " time	*138.5	151.0	157.0	166.0	107.5	-	-	-	-	*87.0	µsecs	
3rd peak volts	-	196	194	-	228	239	243	-	275	-	volts	
" " time	*323.0	304.5	248.0	-	235.5	246.0	306.5	-	279.5	-	µsecs	

* taken from breech voltage record : no muzzle voltage readings Error in time: ± 0.5 µsecs

\+ Note Standard Deviation. Number of samples < 10

\- unable to determine

5.4 Breech Voltage

As shown in Fig. 12 the form of the breech voltage curve is initially similar to that for the muzzle voltage. However, once the plasma is established the breech voltage rises steadily until the plasma leaves the launcher as indicated by the sharp rising exit peak. The rise in the voltage is due to increasing impedance of the launcher as the projectile travels away from the breech and to the back emf generated by the accelerating projectile (see equation on Fig. 12).

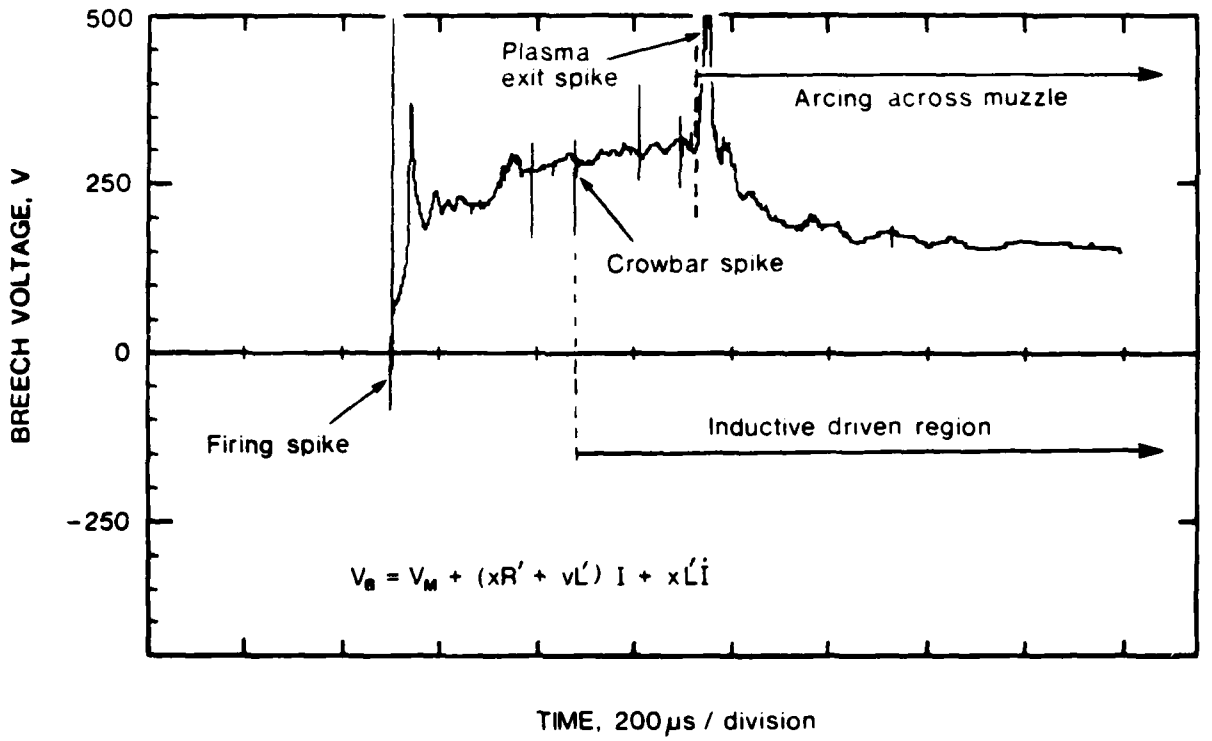

FIGURE 12 Breech voltage record for firing No. 5. Initial Capacitor was 4.2 kV

5.5 Position Coils

Inductive pick-up coils were placed on top of the launcher to provide a displacement-time profile of the projectile flight within the bore, similar to the system used by Barber [2]. These coils were made by winding 20 turns of 38 G(B&S) double enamelled copper wire onto a 1 mm length of a 6 mm diameter nylon former.

As shown in Fig. 13 every second coil was interlinked to form two sets of three coils. Separation between coils was 100 mm, with the first coil 290.5 mm from the rear end of the projectile at its starting position.

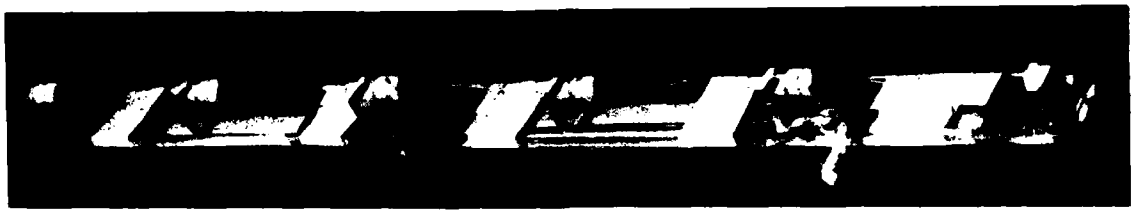

FIGURE 13 Photograph of pick-up coils

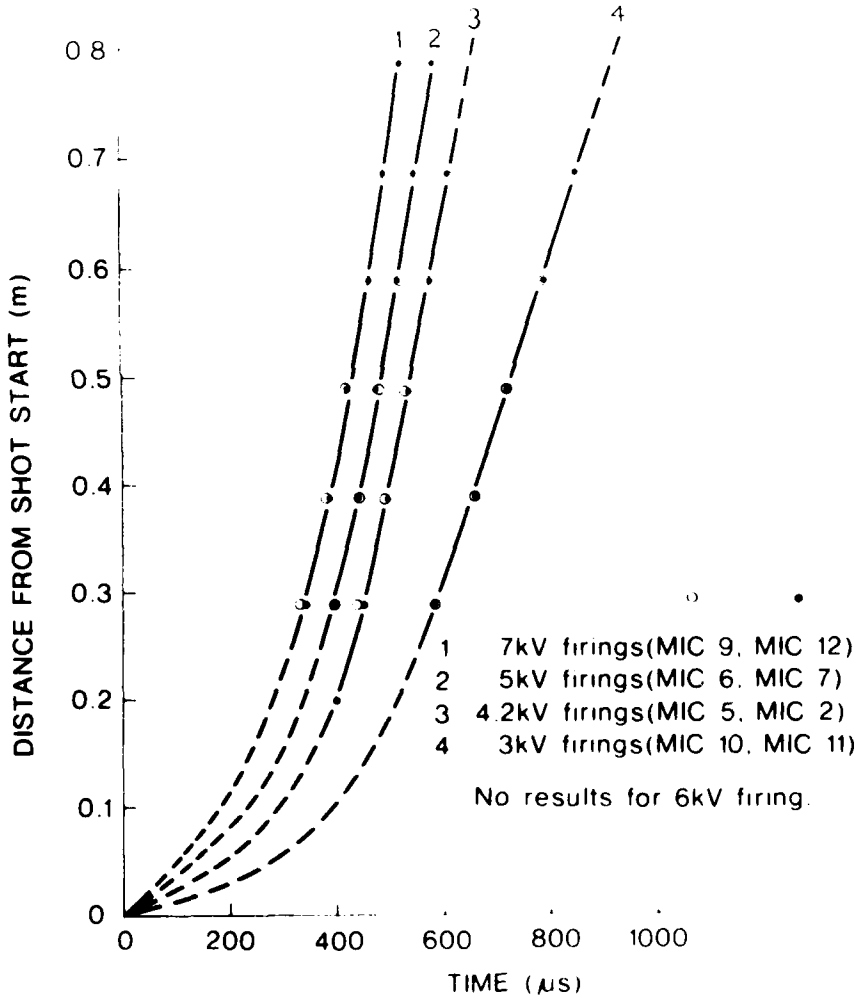

FIGURE 14 In bore position of projectile versus time.
Note: Each curve is the best fit of the results from 2 firings. Repeatibility was excellent.

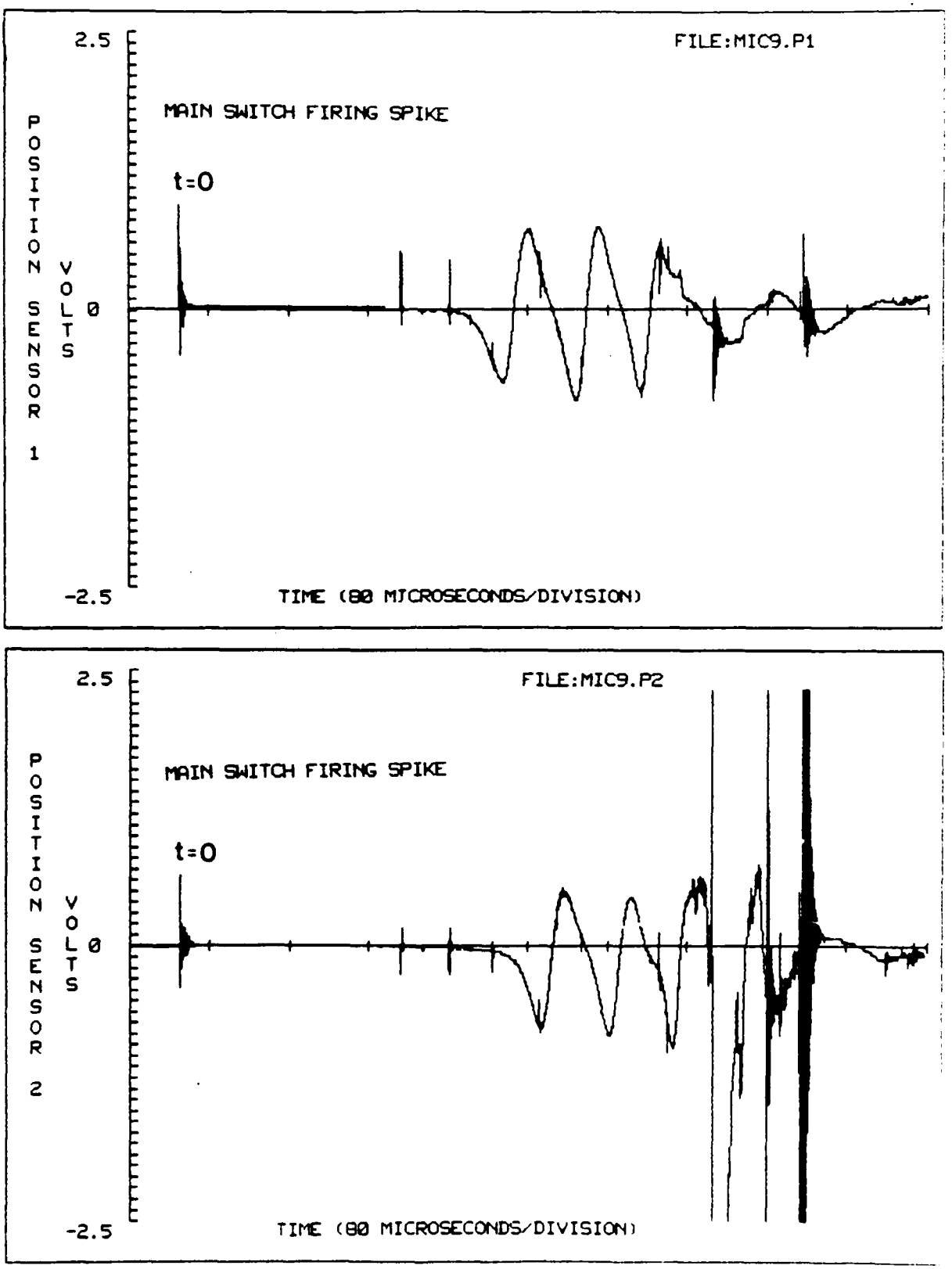

FIGURE 15 Pick-up coil records for firing No. 9

In Figure 14 the crossover times for each position sensor are plotted. Correlation between the two records from the pick up coils was made by the firing and other spurious spikes on the record (fig 15). Jamison [8] reported that the crossover appears to be the current centroid in the armature. Therefore, all the displacement - time curves will include a small error which is dependent on the position of the current centroid behind the projectile.

The maximum acceleration has occurred in the first 290 mm of the launcher, and after this point velocity in each firing remains fairly constant. The lack of significant projectile acceleration after the first 290 mm (although current levels were still high) indicates that significant friction had developed between the projectile and the bore at the high velocities to a value equal or just less than the electromagnetic force (if one assumes that the position of the current centroid relative to the projectile is constant).

6. DATA ANALYSIS

The digital records of voltage and current were used to calculate instantaneous power levels which were integrated to yield the energy dissipation with respect to time. The following definitions were made:-

(a) Instantaneous Power Levels

(1) Breech power = Breech voltage*Current

(2) Muzzle power = Muzzle voltage*Current

(3) "Rail" power = (Breech Voltage-Muzzle Voltage)*Current

(b) Energy dissipation is the time integral of the curves for (1), (2) and (3)

The "rail" energy has four components:-

(1) Magnetic field of the rails

(2) Heating of the rails (resistive and magnetic)

(3) Stress and strain within the rails and the launcher body

(4) Projectile kinetic energy

(c) We define system and launcher efficiencies as follows;

(1) System efficiency $= \frac{\text{Projectile kinetic energy}}{\text{Total energy dissipated}}$

(2) Launcher efficiency $= \frac{\text{Projectile kinetic energy}}{\text{Energy supplied up to time of plasma exit}}$

The energy supplied up to the time of the plasma exit was measured from the breech energy dissipation curves. Figure 16 is the curve for firing number 1 (6 kV). These curves give a measure of the actual energy delivered to the launcher by the power source during acceleration of the projectile. The time interval from the start of the muzzle (or breech) voltage record to the start of the exit spike was considered to be the flight period of the projectile within the bore of the launcher. It was the energy delivered during this interval to the launcher that determined the exit velocity of the projectile. Energy delivered after this period was dissipated in the rails and across the muzzle.

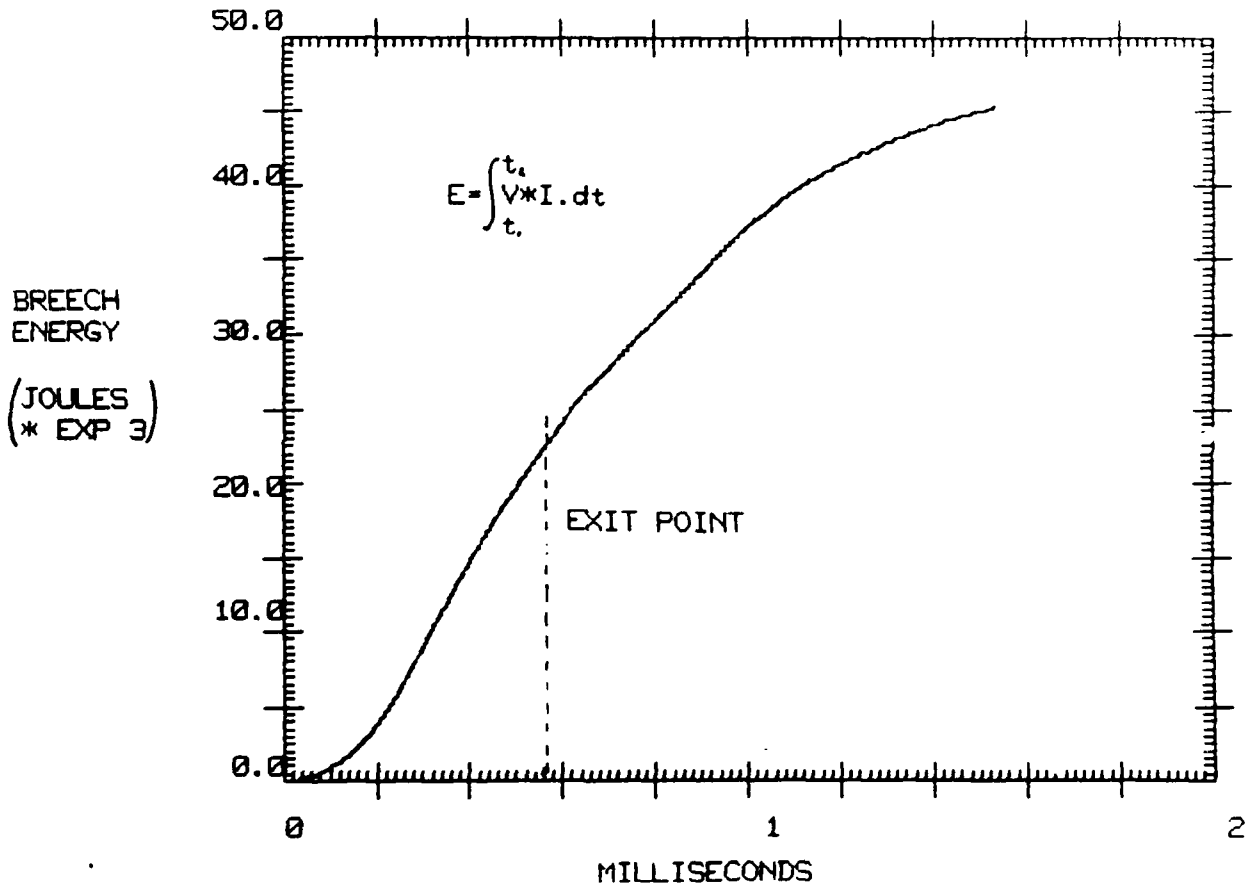

FIGURE 16 Energy delivered to breech of railgun with respect to time. Firing No. 1, Initial Capacitor Voltage 6.0 kV.

Table 3 (page 10) is a compilation of data and calculated values for each of the firings. Total energy expended was calculated using the initial and residual voltage; Breech energy was calculated as explained in (a) and (b) above, projectile velocity is the value calculated from the ballistic pendulum and this is used to calculate the projectile kinetic energy. The system and launcher efficiencies given are those calculated as explained above.

6.1 Energy Distribution

Confining ourselves to that period of the discharge when the projectile was in the bore of the gun we have tabulated the energy dissipation within the various sections of the launcher, (Table 5) and the energy contained within the magnetic fields of the inductor and the launcher at the instant of plasma exit. The results show that although the energy delivered to ERGS-1M increased by a factor of more than 3, the muzzle energy (energy supplied to armature) and rail energy increased by factors of 2 and 7 respectively. This indicates that as power levels increase, rail losses rather than plasma armature losses will dominate the losses within the launcher. A further breakdown of the rail losses reveals that the magnetic energy stored in the gun increased by a factor of 18 whereas the resistive losses only increased 5 times (the mechanical energy stored was considered neglible).

7. MATERIAL DAMAGE

7.1 Rails

The rails were removed after each firing and they relaxed into a lengthwise curvature, concave on the bore side. The degree of curvature tended to increase with the increasing power of the firing. Immediately about the initial position of the projectile there was significant surface melting of the rails whereas, at the muzzle end there was a feather like marking of arc pits on the rail surface. A detailed analysis of the rail damage will be presented in a separate report [9].

7.2 Vulcanised Fibre Rail Separators

The vulcanised red fibre was not replaced during the 12 firings. Unlike the copper rails there was no raised surface damage that would have prevented the passage of another projectile. There was some surface discolouration with some small pitting and erosion. The surface discolouration was due to the resin being removed revealing the lighter coloured cellulose fibres. The original surface texture was not greatly altered by the firings which means the dielectric material experiences only mild surface temperatures and stresses.

7.3 Projectile

Projectiles recovered from the cotton wool packing of the ballistic pendulum had usually broken up into several pieces. However a single hole in the paper witness screen on the front of the ballistic pendulum indicated that the projectile had remained intact during the firing and breakup occurred during deceleration in the pendulum. The pendulum face was 2 m from the

T A B L E 5

ENERGY DISSIPATION AND DISTRIBUTION AT EXIT OF PROJECTILE

Firing Number	Total Energy Expended (kJ)	Energy in† Inductor ($\frac{1}{2}LI^2$) (kJ)	Energy Supplied to Breech (kJ)	Energy in* Inductance of gun (kJ)	Energy Supplied to Armature (kJ)	Energy supplied to Rails (kJ)	Kinetic Energy of Projectile (kJ)
10	27.8	3.2	9.1	0.26	-	-	0.34
11	28.0	3.4	8.9	0.28	7.3	1.6	0.34
2	54.8	14.9	12.9	1.2	8.6	4.4	1.13
5	54.1	22.8	13.4	1.4	8.9	4.5	0.97
6	76.7	29.6	17.4	2.4	10.1	7.3	1.22
7	76.7	29.0	18.2	2.3	10.9	7.3	1.17
1	112.1	40.9	22.7	3.3	14.0	9.1	1.27
3	111.8	40.9	-	3.3	12.11	-	1.60
9	150.3	62.6	28.3	5.1	-	-	1.63
12	149.4	54.9	26.0	4.4	14.8	11.3	0.93

Error in calculations ± 11%

\- Breech and/or muzzle voltage not recorded.

* Inductance of assembled launcher with shorting link (at 909 Hz) = 0.51 μH.

† Inductance of storage inductor = 6.3 μH.

@ See previous definition of rail energy.

muzzle and projectiles travelled through air for this distance. Hole shape variations on the witness screens indicated that the projectiles were tumbling.

7.4 Launcher Body

Cracking of the launcher body after several firings occurred at the muzzle end, (fig. 18). Dissection of the cracked body revealed a section within the laminations where the epoxy resin had not penetrated at manufacture. This weaker section therefore separated due to the stresses of firing.

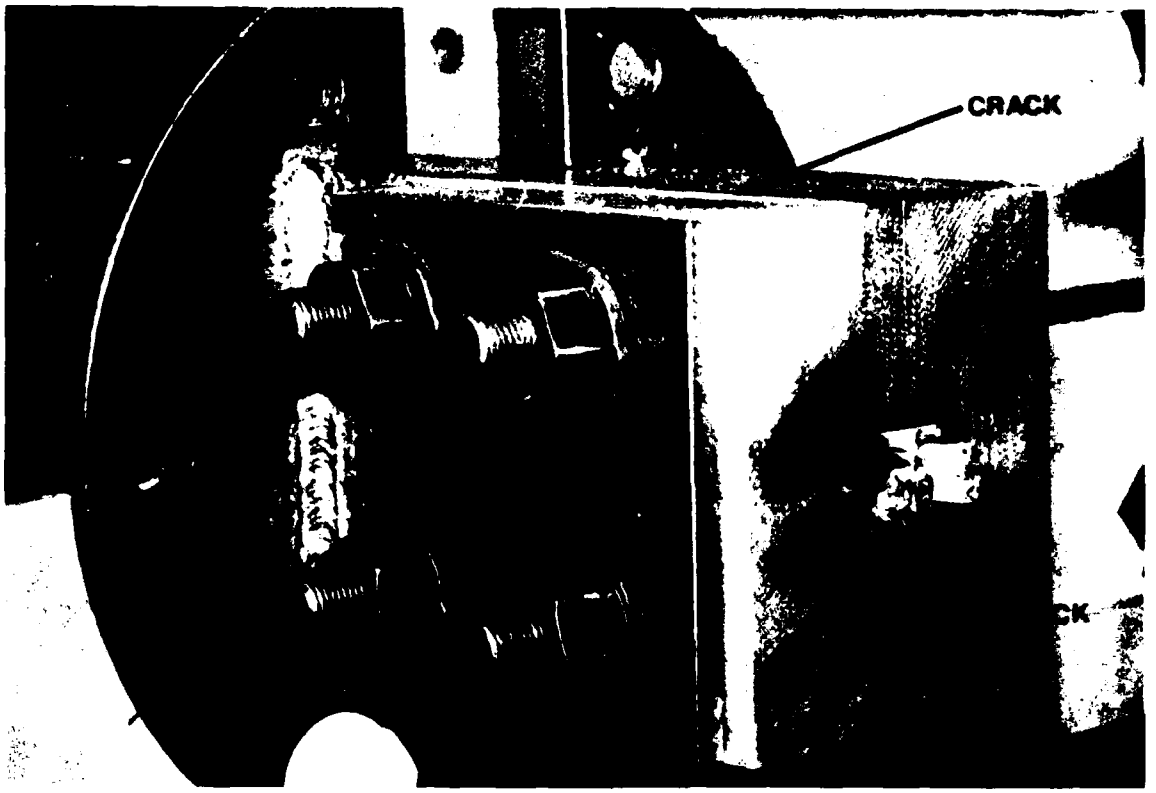

FIGURE 17 Photograph of cracked body at muzzle end of the ERGS-1M railgun

8. DISCUSSION

Although system efficiency was low, the experiments demonstrated a launcher efficiency as high as 8.8%. It is believed that both these figures can be improved in the existing launcher. The main factors affecting efficiencies are (1) energy dissipation in the circuit resistance, (2) dissipation at the muzzle after the exit of the projectile, (system efficiency only) and (3) dissipation in the switches. Item (1) can be reduced with a more efficient inductor and improved coupling of the launcher to the system. To reduce the amount of muzzle arcing, greater attention is required in shaping the current pulse in order to maximise the energy transfer to the projectile. To achieve this in a single or multiple segmented launcher pulse

forming networks may be required. The switching for the launcher would be improved by positioning the main switch on the capacitor bank side of the crowbar switch. This will remove the main switch voltage drop from the circuit after the instant of crowbar and improve the system efficiency. The system efficiency would also be improved if the energy dissipation in the switches was reduced.

The remaining factors concerning the efficiency are the muzzle voltage losses and the rail losses. Lowering the muzzle voltage, which is large in comparison to solid armature muzzle volts, will improve the efficiency but it must be noted that it is a relatively stable value and no methods are yet apparent to make significant reductions. Increases in the current do not produce equivalent increases in the muzzle volts. The rail losses reveal that long single segment railguns will waste energy resistively and/or by storing it in the magnetic field of the gun. The results indicate that the concepts of multiple segmented railguns or distributed energy railguns [11,12] would be more efficient in this aspect.

The experimental diagnostics worked exceptionally well providing very clean records. Simple inbore measurements of the projectile position using position coils proved to be very reliable. Accordingly, it is planned to incorporate coils over the full length of future launchers to record the whole period of acceleration. If electromagnetic interference becomes a problem for the coils at higher energies, the more intricate method of in-bore trip wires, as used by Deis et al [10], may provide a more noise immune system.

In quantifying the circuit parameters, measurement of the L' of the assembled launcher revealed that it varied from 0.60 μH/m to 0.41 μH/m over the frequency range 451 Hz to 20.0 KHz. The presence of such deviations will have to be considered in future simulation codes and experiments, especially for segmented or distributed energy launchers, as these launchers will require pulses of power whose frequency will increase as the projectile accelerates towards the muzzle.

Examination of the launcher after the firings revealed that the vulcanised red fibre was very robust. It is interesting to note the contrast in damage between the red fibre and the melted and bowed rails. Both were apparently subjected to the same extremes of pressure and temperature of the plasma armature as it accelerated along the bore. Thus, the severe damage incurred by the rails was from the passage of current across the rail plasma interface and not from the transient contact of the plasma itself. More theoretical and experimental study is required in this area to explain the behaviour of the plasma armature and the transfer of current between it and the conducting rails.

9. CONCLUSIONS

A small calibre railgun has been successfully used to propel 0.3 g polycarbonate projectiles up to 3.3 km/s from which firings quite extensive diagnostic data were extracted.

We have observed fairly steady armature voltage characteristics during projectile accelerations and have indications that the average value of this steady armature voltage is dependent on energy input to the railgun.

Calculation of acceleration in the bore of the railgun from pick-up coil readings have indicated that friction losses in the bore of small calibre railguns is sufficient to reduce acceleration to zero about 300 mm after shot start.

Some calculations have been done to provide a measure of railgun efficiency for the present firings and show that actual transfer of energy in the railgun during projectile acceleration varied between about 3.5 and 9%. The major losses occur in the magnetic field and resistances of the railgun and circuit, and by frictional losses in the railgun.

10. ACKNOWLEDGEMENTS

The electromagnetic research program at Materials Research Laboratories has been assisted by support from the US Defense Advanced Research Projects Agency (DARPA). The authors are grateful for this support, in particular to Dr H.D. Fair Jr. of DARPA.

We also sincerely thank Dr Y.C. Thio, formerly of MRL, now at Westinghouse R. & D. Center, whose theoretical and design concept work was the foundation for the research results presented herein.

Thanks are also due to our colleagues who assisted in design and experimentation; D. Sadedin, D. Stainsby, A. Jenkins, J. Thomas, B. Jones and M. Astill. We particularly thank Dr R.A. Marshall for his comments and suggestions during the formulation of this report.

11. REFERENCES

1. Rashleigh, S.C. and Marshall, R.A. Electromagnetic Acceleration of Macroparticles to High Velocities. J. Appl. Phys. 49, (4), 1978.

2. Barber, J.P. The Acceleration of Macroparticles and a Hypervelocity Electromagnetic Acceleration. PhD Thesis EP-T12 Australian National University 1972.

3. 1980 Conference on Electromagnetic Guns and Launchers IEEE Transactions on Magnetics, January, 1982 Vol. MAG-18 No. 1.

4. Thio, Y.C. PARA: A Simulation Code for plasma driven electromagnetic launchers. MRL-R-873, 1983.

5. Bedford, A.J., Clark, G.A. and Thio, Y.C. Experimental Electromagnetic Launchers at MRL. MRL-R-894, 1983.

6. Clark, G.A., and Thio, Y.C. Design and Operation of a Self-Activating Crowbar Switch. EML Conference Proceedings, Boston, Massachusetts, Oct 10-13, 1983. To be published IEEE transactions on Magnetics.

7. Richardson, D.D. and Marshall, R.A. Use of the Computer Program PARA-80 to study results from firing the railgun ERGS-IM. MRL-R-900, 1983.

8. Jamison, K.A. Arc Armature Experiments and Other B.R.L. Activities. DARPA Electromagnetic Launcher Review 29-30 Sept 1982, unpublished conference document.

9. Bedford, A.J. Rail Damage in a Small Calibre Railgun. EML Conference Proceedings, Boston, Massachusetts, Oct 10-13, 1983. To be published IEEE transactions on Magnetics.

10. Deis, D.W. and Ross, D.P. Experimental Launcher Facility-ELF-1: Design and Operation. IEEE Trans on Mag. Vol. Mag-18, No.1, January 1982.

11. Parker, J.V. Electromagnetic Projectile Acceleration Utilising Distributed Energy Source. J. Appl. Phys. 53(10) October 1982.

12. Marshall, R.A. and Stump, W.R. The CEM-UT Distributed Energy Store Railgun. Report on the two stage version Publication No. R0-9 Centre for Electromechanics, University of Texas at Austin, Texas, U.S.A.

APPENDIX A

ROGOWSKI BELT CONSTRUCTION

A Rogowski belt permits non-intrusive measurement of an alternating current in a circuit. (See Appendix B for theory)

The belt used during the experiments was constructed from a 470 mm length of RG58 coaxial cable. The outer sheath and copper braid were removed and 21G(B&S) double enamel copper wire was closely wound onto the polyethylene insulation over the entire length giving approximately 13 turns/cm. Heat shrink tubing was placed over the windings to hold them in place. At one end, the winding was terminated to the central conductor in the polyethylene. The opposite end of the belt was mounted into a small perspex block on which an isolated BNC (RG47) connector had been attached. The central conductor and the winding terminations were soldered to the centre and shield tabs of the connector respectively. The winding was curved and held in a circle by fitting the unattached end of the belt into the same perspex block and clamping it in place with a nylon screw, (fig. A1).

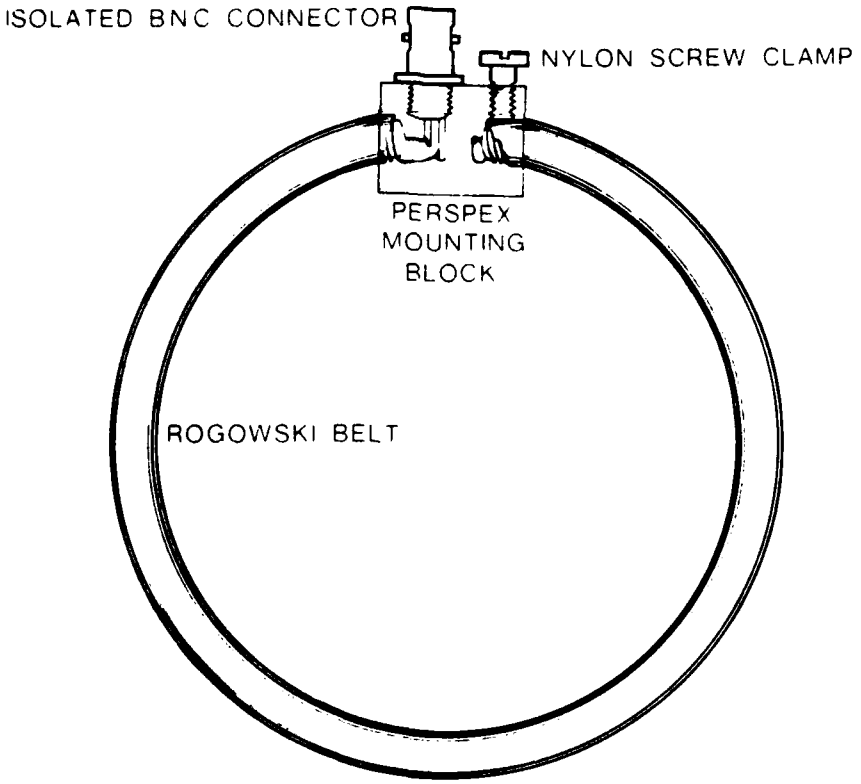

FIGURE A1. Rogowski Belt Experimental Arrangement

APPENDIX B

ROGOWSKI BELT SIGNAL CORRECTION

Simple theory

In its simplest form a Rogowski belt is a toroidal coil placed around a current carrying conductor, (Fig. B1).

The changing magnetic field B around the conductor causes a changing flux in the loops of the Rogowski belt. The voltage V induced in the belt is given by:-

$$V = \int \frac{N}{\ell} \, d\ell \, \frac{d}{dt} \iint_S \mu H dS$$

N = No of turns in coil

ℓ = length of coil

S = X'sectional area of turn

H = magnetic field strength

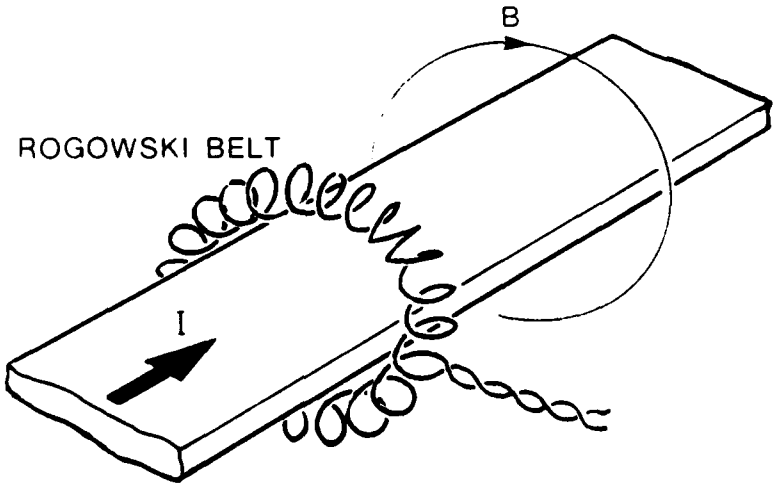

FIGURE B1. A Simple Toroidal Rogowski Belt Around a Conductor

Using Stoke's theorem and Ampere's law this equation reduces to:-

$$V = \frac{N}{\ell} S\mu \frac{dI}{dt}$$

$$= k \frac{dI}{dt} \qquad \text{where } k = \text{constant}$$

Thus the signal coming from the Rogowski belt is the first derivative of the current flowing in the conductor.

A detailed analysis of Rogowski belts is given by Knoepfel [B1].

Experiment

In order to record the current and not the derivative, the Rogowski belt signal was passed through a simple RC integrator which was attached to the input of the transient recorder.

Analysing this RC network (fig. B2) the following equation is derived.

$$V_R + \tau \frac{dV_R}{dt} = bV_{in} \qquad (1) \qquad \text{where: } \tau = bR\,C \qquad b = \frac{R_R}{R_R + R}$$

Integrating (1) w.r.t. time and dividing by τ we get

$$V_R + \frac{1}{\tau} \int V_R dt = \frac{1}{R\,C} \int V_{in} dt$$

Here V_R was recorded and the term $\frac{1}{\tau} \int V_R dt$ is an error term. τ was not sufficiently large in the integrator that this term could be neglected. This error component was calculated from the digitised record of V_R and added to it to obtain the corrected record.

References:

B1. Knoepfel, H. Pulsed High Magnetic Fields. North Holland Publishing Co., 1970, ISBN 0 444 100 350.

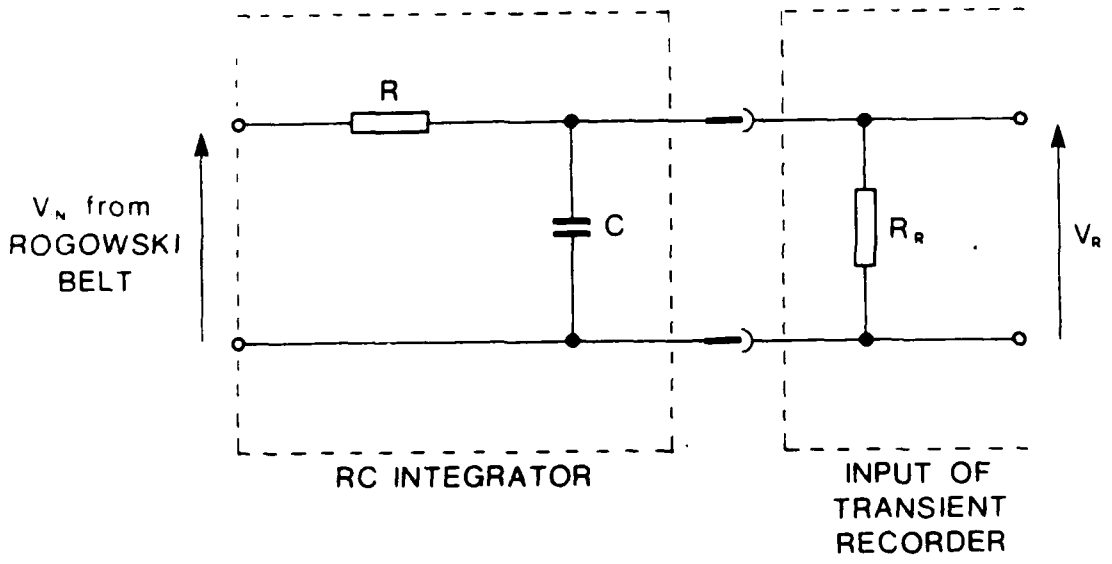

FIGURE B2. Integrator Circuit Used in Conjunction with Rogowski Belt (R = 110 kΩ, C = 100 nF, R_R = 1 MΩ)

(MRL-R-917)

DISTRIBUTION LIST

MATERIALS RESEARCH LABORATORIES

Director
Superintendent, Physical Chemistry Division
Dr J. Eadie
Library (2 copies)
G.A. Clark
Dr A.J. Bedford (5 copies)

DEPARTMENT OF DEFENCE

Chief Defence Scientist (for CDS/DCDS/CPAS/CERPAS) (1 copy)
Superintendent, Science and Administration
Army Scientific Adviser
Air Force Scientific Adviser
Navy Scientific Adviser
Officer-in-Charge, Document Exchange Centre (17 copies)
Technical Reports Centre, Defence Central Library
Deputy Director, Scientific and Technical Intelligence,
Joint Intelligence Organisation
Librarian, Bridges Library
Librarian, Engineering Development Establishment
Defence Science Representative (Summary Sheets only)
Australia High Commission, London
Counsellor Defence Science, Washington, D.C. (Summary Sheets only)
Librarian (Through Officer-in-Charge), Materials Testing
Laboratories, Alexandria, NSW
Senior Librarian, Aeronautical Research Laboratories
Senior Librarian, Defence Research Centre Salisbury, SA
Defense Attache, Australian Embassy, Bangkok, Thailand
(Att. D. Pender)

DEPARTMENT OF DEFENCE SUPPORT

Deputy Secretary, DDS
Head of Staff, British Defence Research & Supply Staff (Aust.)

OTHER FEDERAL AND STATE DEPARTMENTS AND INSTRUMENTALITIES

NASA Canberra Office, Woden, ACT
The Chief Librarian, Central Library, CSIRO
Library, Australian Atomic Energy Commission Research Establishment

DISTRIBUTION LIST
(continued)

MISCELLANEOUS - AUSTRALIA

Librarian, State Library of NSW, Sydney NSW
University of Tasmania, Morris Miller Lib., Hobart, Tas.

MISCELLANEOUS

Library - Exchange Desk, National Bureau of Standards, USA
UK/USA/CAN/NZ ABCA Armies Standardisation Representative (4 copies)
Director, Defence Research Centre, Kuala Lumpur, Malaysia
Exchange Section, British Library, UK
Periodicals Recording Section, Science Reference Library, British Library, UK
Library, Chemical Abstracts Service
INSPEC: Acquisition Section, Institute of Electrical Engineers, UK
Engineering Societies Library, USA
Aeromedical Library, Brooks Air Force Base, Texas, USA
Ann Germany Documents Librarian, The Centre for Research Libraries, Chicago, Ill.

ADDITIONAL DISTRIBUTION

DARPA/TTO, 1400 Wilson Boulevard, Arlington, VA 22209, USA (Attn. Dr H.D. Fair Jr)
AMCCOM, ARDC- Dover NJ 07801, USA, Building 382 (Attn. Dr P.J. Kemmey, Dr T. Gora)
AMCCOM, ARDC- Ballistics Research Laboratory DRDAR-BLB, Aberdeen Proving Ground, MD 21005, USA (Attn. Dr D. Eccleshall, Dr J.D. Powell, K.A. Jamison)
Naval Surface Weapons Center (NSWC/DL), Dahlgren VA 22448, USA (Attn. Dr M.F. Rose Code F-04, Dr H.B. Odom Code F-12)
Naval Research Laboratory, Code 4770, Washington DC 20375, USA (Attn. Dr R. Ford)
US Air Force, Armament Laboratory (AFATL/DLDB), Eglin Air Force Base FL 32542, USA (Attn. Dr W. Lucas)
US Air Force, Aero Propulation Laboratory, Power Division (AFWAL/POOS-2) Wright-Patterson Air Force Base OH 45433, USA (Attn. Dr C. Oberly)
US Air Force, Office of Scientific Research, Bolling AFB, Washington, DC 20332, USA (Attn. Dr L. Caveny)
US Air Force, Rocket Propulsion Laboratory, Edwards AFB CA 93523 (Attn. LKDH/Lt Phil Roberts)
NASA, Ames Research Centre, Moffet Field CA 94035, USA (Attn. Technical Library)
NASA, Langley Research Center, Langley Field Station, Hampton VA 23365 USA (Attn. Technical Library)

DISTRIBUTION LIST
(continued)

ADDITIONAL DISTRIBUTION (contd)

NASA, Lewis Research Center, Cleveland OH 44135, USA
(Attn. William R. Kerslake)
NASA, Goddard Space Flight Centre, Greenbelt MD 20771, USA
(Attn. Technical Library)
NASA, Scientific and Technical Information Facility, Baltimore MD 21240
USA (Attn. Accessioning Department)
Jet Propulsion Laboratory, 4800 Oak Grove Drive, Pasadena CA 91102, USA
(Attn. Technical Library)
Batelle Columbus Laboratories, 505 King Avenue, Columbus OHIO 43201, USA
(Attn. Dr Eric Rice)
General Dynamics, P.O. Box 2507, Pomona, CA 91769, USA
(Attn. Dr J.H. Cuadros (44-21)
International Applied Physics, Research, 7546 McEwen Road, Dayton,
Ohio 45459, USA (Attn. Dr J.P. Barber)
Lawrence Livermore National Laboratories, PO Box 808, Livermore CA 94550
USA (Attn. Dr Ron Hawke)
Litton Industries, 360 North Crescent Drive, Beverly Hills CA 90210, USA
(Attn. Dr R. Salter, Dr J. Scudder)
Los Alamos National Laboratory, Mail Stop 970, Los Alamos NM 87545, USA
(Attn. Dr Max Fowler)
Los Alamos National Laboratory, Mail Stop 525, Los Alamos NM 87545, USA
(Attn. Dr Gerry Parker)
Los Alamos National Laboratory, Mail Stop 985, Los Alamos NM 87545, USA
(Attn. Dennis Peterson)
Massachusetts Institute of Technology, Francis Bitter National Magnet
Laboratory, Cambrdige MA 02139, USA (Attn. Dr H. Kolm)
Physics International Company, 2700 Merced Street, San Leandro CA 94577
USA (Attn. Dr Ed Goldman)
Science Applications Inc. 1503 Johnson Ferry Road (Suite 100),
Marietta, GA, 30062, USA (Attn. Dr J.H. Batteh)
University of Texas at Austin, Center for Electromechnics (CEM),
Austin TX 78712, USA (Attn. Dr William Weldon)
Vought Corporation, Advanced Technology Center, PO Box 226144,
Dallas TX 75266, USA (Attn. Dr C.H. Haight, Dr Mike Tower)
Westinghouse Electric Corporation, 1310 Beulah Road, Pittsburgh PA 15235
USA (Attn. Mr C.J. Mole, Dr I. McNab, Dr D.W. Deis, Dr Y.C. Thio)
Westinghouse Electric Corporation, Sunnyvale CA 94088, USA
(Attn. Mr William A. Volz)
Sandia Laboratories, Albuquerque NM 87115, USA (Attn. Dr M. Cowan)
Rand Corporation, Santa Monica CA, USA (Attn. Dr Gerald A. Sears
Dr William J. Whelan)
General Atomics, San Diego CA, USA (Attn. Dr Sibley Burnett)
JAYCOR, 205 South Whiting Street, Alexandria VA 22304, USA
(Attn. Dr Derek Tidman)
General Electric Company, Schenectady, NY, USA
(Attn. Mr Robert A. Marshall)
Research School of Physical Sciences, Australian National University,
Box 4, PO, Canberra ACT 2601 (Attn. Prof S. Kaneff)

DISTRIBUTION LIST
(continued)

ADDITIONAL DISTRIBUTION (contd)

Counsellor Defence Science, Australian Embassy, Washington
(Attn. Mr R.A. Cummins)
Professor A.E. Guile, Dept. of Electrical and Electronic Engineering,
The University of Leeds, Leeds LS2 9JT, England

DOCUMENT CONTROL DATA SHEET

REPORT NO.	AR NO.	REPORT SECURITY CLASSIFICATION
MRL-R-917	AR-003-898	UNCLASSIFIED

TITLE

PERFORMANCE RESULTS OF A SMALL-CALIBRE ELECTROMAGNETIC LAUNCHER

AUTHOR(S)

G.A. CLARK
A.J. BEDFORD

CORPORATE AUTHOR
Materials Research Laboratories
P.O. Box 50,
Ascot Vale, Victoria 3032

REPORT DATE	TASK NO.	SPONSOR
FEBRUARY 1984	DST 82/212	DSTO

CLASSIFICATION/LIMITATION REVIEW DATE

CLASSIFICATION/RELEASE AUTHORITY
Superintendent, MRL
Physical Chemistry Division

SECONDARY DISTRIBUTION

Approved for Public Release

ANNOUNCEMENT

Announcement of this report is unlimited

KEYWORDS

Electric guns Railguns

COSATI GROUPS 2103 1906

ABSTRACT

Results of electromagnetic launcher experiments are presented. Using an inductor and a crowbarred capacitor bank, 0.3 g projectiles have been accelerated over 800 mm to a velocity of 3.3 km/s. Voltage, current, power and energy curves are presented, as are tables of muzzle volts and efficiencies. The launcher design, circuit parameters and instrumentation are detailed and discussed. The report has been presented in a manner such that the data may be used by others to test theoretical work and to compare with experiments on other systems.